Received: 2 March 2016 | Revised: 10 April 2016 | Revised: 10 April 2016

DOI: 10.37917/ijeee.12.1.5 | Vol. 12| Issue 1 | June 2016

Open Access

Iraqi Journal for Electrical and Electronic Engineering

Original Article

IJEEE University of Basrh College of Engineering

Finite Control Set Model Predictive Current Control FCS-MPC Based on Cost Function Optimization, with Current Limit Constraints for Four-Leg VSI

Riyadh G. Omar
Department of Electrical Engineering
University of Al-Mustansiriyah
Riy68gh@yahoo.com

Rabee' H. Thejel
Department of Electrical Engineering
University of Basra
Rabee_alabbasi@ieee.org

Abstract— A Matlab/Simulink model for the Finite Control Set Model Predictive current Control FCS-MPC based on cost function optimization, with current limit constraints for four-leg VSI is presented in this paper, as a new control algorithm. The algorithm selects the switching states that produce minimum error between the reference currents and the predicted currents via optimization process, and apply the corresponding switching control signals to the inverter switches. The new algorithm also implements current constraints which excludes any switching state that produces currents above the desired references. Therefore, the system response is enhanced since there is no overshoots or deviations from references. Comparison is made between the Space Vector Pulse Width Modulation SVPWM and the FCS-MPC control strategies for the same load conditions. The results show the superiority of the new control strategy with observed reduction in inverter output voltage THD by 10% which makes the FCS-MPC strategy more preferable for loads that requires less harmonics distortion.

Index Terms—current control, current constraint, finite set, four-leg inverter, model predictive control, SVPWM.

I. INTRODUCTION

In the last few years, predictive control took a large interest in the design of modern power electronics controllers. The principle of operation of this type of control depends on the system model, to predict the next action of the controlled variables, and then the controller uses this prediction with predefined optimization process to compute optimal control commands.

Many advantages made the predictive control more attractive to control power converters, the simple principle of operation, easy to achieve, and it can be implemented with various types of voltage source converters, as a drawback it needs a large number of calculations, but using high speed computers can solve this problem. The predictive control strategies can be classified into:

1. Hysteresis predictive control.
2. Trajectory predictive control.
3. Dead beat predictive control.
4. Model predictive control.

Model Predictive Control (MPC) represents a more flexible approach when compared to the other three types, because it uses a minimization cost function and it doesn't require a modulator to generate the desired voltage.

Model Predictive Control (MPC) represents a more flexible approach, because it uses a minimization cost function and it doesn't require a modulator to generate the desired voltage[1]. Related to the advantages of MPC over other classical control methods; it is employed widely in controlling traditional power converters

besides multilevel converters [2-4]. The main factor that distinguishes the MPC, is the necessity to deal with one control loop (load currents), where the error between the predefined references and the predicted values of load currents is minimized. In this work, finite control set MPC strategy with current constraints is presented to control the four-leg VSI.

II. FINITE CONTROL SET MPC (FCS-MPC) OPERATION PRINCIPLE

In power converter, the discrete nature of the signal is obvious in its work; a finite number of switching states is used to produce the desired output. The MPC simply predicts the next action of the system, according to each possible switching state; these predictions are then used to calculate a cost function in optimization process. Eventually, the switching state that gives the minimum error (i.e. minimum cost function) is selected as a switching command. This process is called Finite Control Set MPC (FCS-MPC)[5]. The control problem of the voltage source inverter can be reduced to find the proper switching action S(t), this action is the gate switching command signals. These signals produce the system variable y(t), which is close to the required reference y*(t). If $y(t_k)$ is the value of y(t) during the sample time T_s, and considering a finite number of switching control actions of (n), Fig.1 shows the FCS-MPC operation principle[1,5]. S_i is the switching control action, where (i=1,…., n), $y(t_k)$ is the measured value, $y_{pi}(t_k+1)=f_p\{y(t_k),S_i\}$ for (i=1,.., n), where f_p is the prediction function which is used to compute all the possible predictions of the system transitions. The prediction function (f_p) is derived from the discrete system model and its parameters. The close switching action to the reference y*(t) is selected in the next step. The comparison is achieved by using a cost (decision) function f_g, which depends on the reference, and the prediction values, and represented by:

$$g_i=f_g\left\{y^*(t_k+1),y_{pi}(t_k+1)\right\} \qquad \text{for i=1,…, n.}$$

When T_s is small enough compared to the system dynamic, the reference value is considered constant during one sample period $y^*(t_k+1) = y^*(t_k)$. The cost function f_g can be represented by the absolute error between the system prediction value and the required reference value. This process leads to (n) cost functions, since there are (n) predictions. Therefore, the switching control action that produces minimum cost function is selected as the command signal.

In Fig.1 the predicted value $y_{p3}(t_k+1)$ is the most proper prediction, since it is the nearest value to the reference value $y^*(t_k+1)$. Accordingly, the switching control signal S_3 that produce $y_{p3}(t_k+1)$ is selected, and applied at this period. Similarly, S_2 which produce $y_{p2}(t_k+1)$ is selected during the next sample time. An FCS-MPC that is included in simple system control block is shown in Fig.2[6].

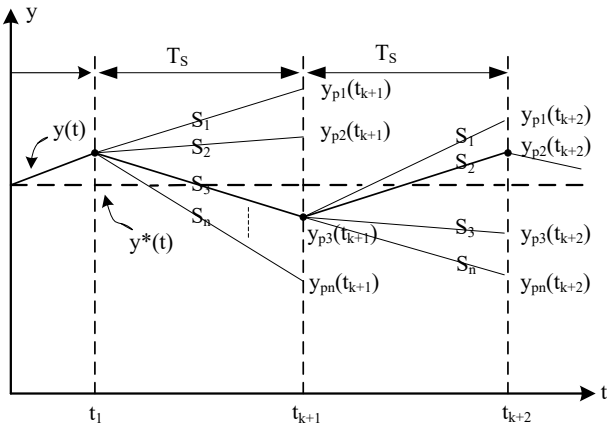

Fig.1 FCS-MPC operation principle.

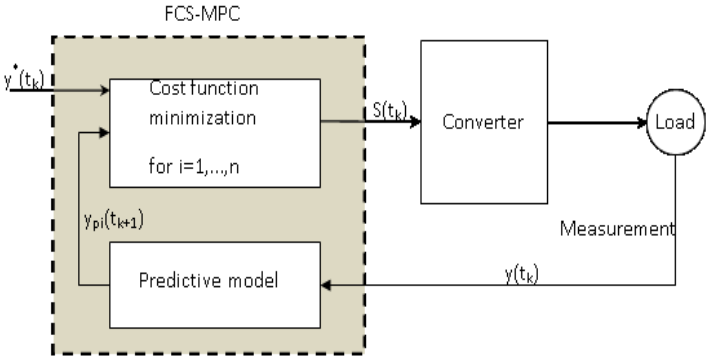

Fig.2 FCS-MPC control block diagram.

III. FOUR-LEG VOLTAGE SOURCE INVERTER MODEL

The Four-leg Voltage Source Inverter VSI represents the best choice when dealing with unbalance and /or non-linear loads. In addition, it provides neutral connection between three-phase load and supply source without using any transformer[7]. This type of inverters has 16 (2^4) of switching states compared with traditional 8 (2^3) switching states in three-leg inverter. Flexibility, the wide range of applications, the good quality of outputs, and the ability of dealing with zero sequence current/voltage, all can be achieved with this type of inverters[8]. The four-leg VSI with L filter and neutral connection is shown in Fig.3. The first step of deriving the mathematical model of the inverter is by describing the dependence of the load voltages on the switching signal commands.

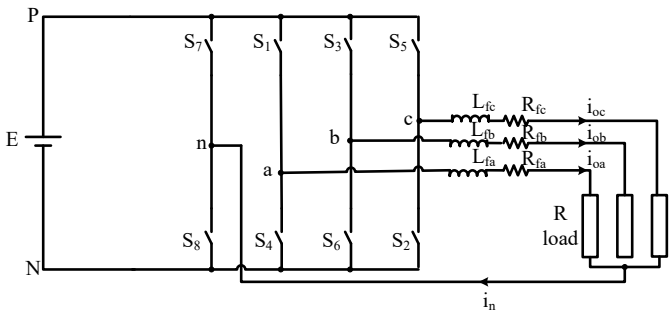

Fig.3 Four-leg VSI topology with L filter.

The inverter switches perform the connection between points P and N (positive and negative of the dc source) and the three-phase load terminals. S_1, S_3, S_5, and S_7 represent four switching control commands, which produces 16 (2^4) switching states[9,10]. These switching states are shown in Table-5.1. The analysis of this type of inverters can be simplified by using resistive load with R-L filter; the control strategy can be extended to more complex loads.

This is shown in Fig.3 where, L_f represents the filter inductance, R_f its resistance, and R is the load resistance. The four-leg voltages are measured with respect to point N (dc source negative point) are:

Table-1Switching states of the four-leg VSI.

Vector	Leg a	Leg b	Leg c	Leg n	V_{an}	V_{bn}	V_{cn}
V_0	0	0	0	0	0	0	0
V_1	0	0	0	1	-E	-E	-E
V_2	0	0	1	0	0	0	E
V_3	0	0	1	1	-E	-E	0
V_4	0	1	0	0	0	E	0
V_5	0	1	0	1	-E	0	-E
V_6	0	1	1	0	0	E	E
V_7	0	1	1	1	-E	0	0
V_8	1	0	0	0	E	0	0
V_9	1	0	0	1	0	-E	-E
V_{10}	1	0	1	0	E	0	E
V_{11}	1	0	1	1	0	-E	0
V_{12}	1	1	0	0	E	E	0
V_{13}	1	1	0	1	0	0	-E
V_{14}	1	1	1	0	E	E	E
V_{15}	1	1	1	1	0	0	0

$$\begin{bmatrix} v_{aN} \\ v_{bN} \\ v_{cN} \\ v_{nN} \end{bmatrix} = \begin{bmatrix} S_1 \\ S_3 \\ S_5 \\ S_7 \end{bmatrix} .E \qquad (1)$$

The inverter output voltages supplied to the filter can be expressed as:

$$\begin{bmatrix} v_{an} \\ v_{bn} \\ v_{cn} \end{bmatrix} = \begin{bmatrix} S_1 - S_7 \\ S_3 - S_7 \\ S_5 - S_7 \end{bmatrix} .E \qquad (2)$$

Applying Kirchhoff's voltage law on the circuit in Fig.3:

$$\left.\begin{aligned} v_{aN} &= (R_{fa}+R_a)i_{oa} + L_{fa}\frac{di_{oa}}{dt} + v_{nN} \\ v_{bN} &= (R_{fb}+R_b)i_{ob} + L_{fb}\frac{di_{ob}}{dt} + v_{nN} \\ v_{cN} &= (R_{fc}+R_c)i_{oc} + L_{fc}\frac{di_{oc}}{dt} + v_{nN} \end{aligned}\right\} \qquad (3)$$

where,

R_{fa}, R_{fb}, and R_{fc} are filter resistances for phases a, b, and c.

L_{fa}, L_{fb}, and L_{fc} are filter inductances for phases a, b, and c.

i_{oa}, i_{ob}, and i_{oc} are the load currents for phases a, b, and c.

Using Eqs.(2) and (3), the inverter output

voltages are:

$$\left.\begin{aligned} v_{an}&=(R_{fa}+R_a)i_{oa}+L_{fa}\frac{di_{oa}}{dt}\\ v_{bn}&=(R_{fb}+R_b)i_{ob}+L_{fb}\frac{di_{ob}}{dt}\\ v_{cn}&=(R_{fc}+R_c)i_{oc}+L_{fc}\frac{di_{oc}}{dt}\end{aligned}\right\} \quad (4)$$

This can be written in a matrix form as:

$$v_o=(R_f+R)i_o+L_f\frac{di_o}{dt} \quad (5)$$

where,

$$v_o=[v_{an}\ \ v_{bn}\ \ v_{cn}]^T$$

$$i_o=[i_{oa}\ \ i_{ob}\ \ i_{oc}]^T$$

$$R_f=[R_{fa}\ \ R_{fb}\ \ R_{fc}]^T$$

$$L_f=[L_{fa}\ \ L_{fb}\ \ L_{cnfc}]^T$$

The neutral current is expressed as follows:

$$i_n=i_{oa}+\ i_{ob}+\ i_{oc} \quad (6)$$

The continuous time load current can be found by solving Eq.(5) as follows:

$$\frac{di_o}{dt}=\frac{1}{L_f}\left[v_o-(R_f+R)i_o\right] \quad (7)$$

IV. FCS-MPC Current Control Based On Cost Function Optimization with Current Constraint.

The finite control set MPC based mainly on optimizing the cost function. This strategy founds large power electronics applications in the last few years, due to its easy concept understanding, high-speed, and the ability to deal with nonlinearities and system constraints[9]. The block diagram of this method is shown in Fig.2. The main steps, which are implemented in this method, are measuring the load current at the kth period, generating a load current reference depending upon the required application, and finally the discrete predictive model is constructed. The discrete model is derived from the continuous model, which is described in the previous section.

In this work the model discretization is achieved by using the first-order approximation for all the derivatives, which results in acceptable accuracy[6,7].

$$\frac{di_o}{dt}=\frac{i_o(k+1)-i_o(k)}{T_s} \quad (8)$$

Substituting Eq.(8) in Eq.(7) results:

$$i_o(k+1)=\frac{T_s}{L_f+(R_f+R)T_s}v_o(k)+\frac{L_f}{L_f+(R_f+R)T_s}i_o(k) \quad (9)$$

Equation (9) shows that, the predictive load current at the (k+1) instant requires load's current measurement, and load voltage at the k^{th} instant. The load voltage $v_o(k)$ depends upon the switching signals, and the d.c source voltage E. The proposed algorithm computes all the 2^4 (16) switching possibilities shown in Table-1 for $v_o(k)$, to obtain sixteen different values of $i_o(k+1)$. The FCS-MPC algorithm selects the switching state in the k^{th} instant, that produces the minimum error between the computed predictive load current $i_o(k+1)$ and the reference load current $i_o^*(k+1)$ at the (k+1) instant. The selected optimal switching state is applied to the system, as a switching control signal through the whole (k+1) period. This comparison process can be achieved by using the cost function (g), which represents the minimum absolute error as follows:

$$\begin{aligned} g(k+1)&=\left\|i_o^*(k+1)-i_o(k+1)\right\|\\ &=\left\|i_{oa}^*(k+1)-i_{oa}(k+1)\right\|+\left\|i_{ob}^*(k+1)-i_{ob}(k+1)\right\|\\ &+\left\|i_{oc}^*(k+1)-i_{oc}(k+1)\right\| \end{aligned} \quad (10)$$

The cost function equal to zero (g=0), when the output load current reaches its reference value. The purpose of the cost function is to reduce the error into zero value. In addition, any constraints such as current limits, switching reduction, etc. can be considered in the cost function, to enhance the system performance. In a dynamic system, when the references obtained at the k^{th} instant, an extrapolation of these references to the next instant (k+1) is applied. This accomplished before using them in the cost function. However, if the sampling time T_s is less than or equal to 20μs, no extrapolation is needed[11], and $i_o^*(k)=i_o^*(k+1)$[7].

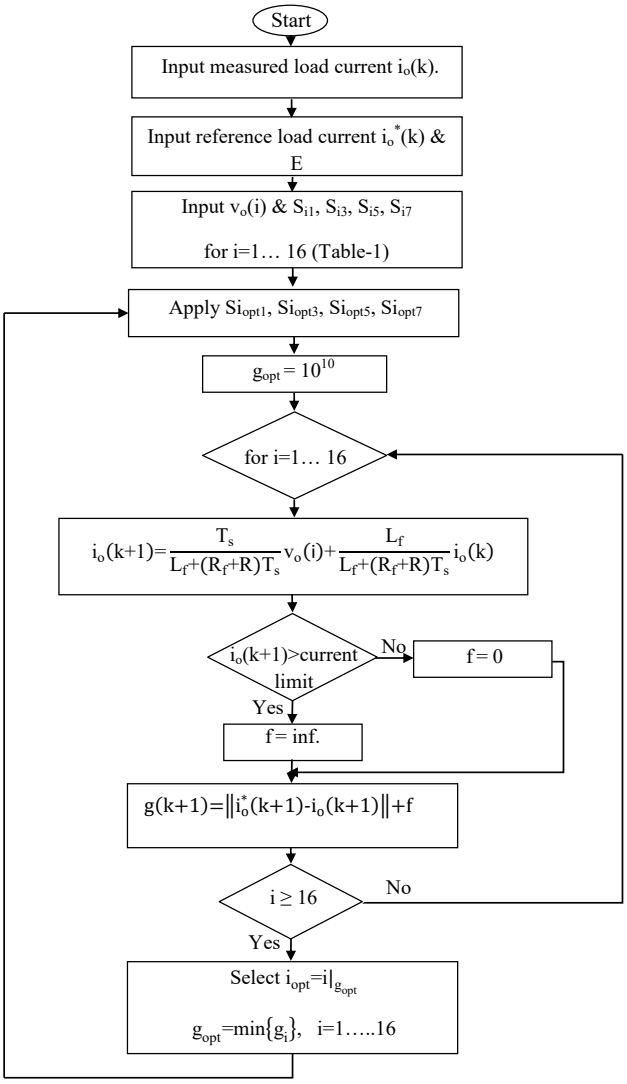

Fig.4 Flow-chart of the current control FCS-MPC algorithm.

A flow-chart of the current control FCS-MPC algorithm is illustrated in Fig.4.

The proposed algorithm can deal with predicted load current limits, by using the function(f) as a cost function constraint, any value of the predicted load current that exceeds the limit, makes the cost function g(k+1) equals to infinity, which result in exclusion of this cost function value and the corresponding switching state from the optimization process.

V. Simulation of FCS-MPC Current Control Based On Cost Function Optimization with Current Constraint for Four-Leg VSI.

The Matlab/Simulink implemented model of the FCS-MPC current control for the four-leg VSI is illustrated in Fig.5. the system parameters are: R_f=0.7Ω, X_f=15mH, R_L=10Ω, T_S=20μsec. The inverter subsystem block, consists of two main subsystems blocks, see Fig.6. The first subsystem is (inverter1), which represents the four-leg inverter. SEMKRON (SKM50GAL12T4) IGBT is selected as a switch, using its current data (fall time, rise time, and tail time) in inverter model (IGBT block) simulation and circuit design. The inner details of this subsystem are shown in Fig.7.

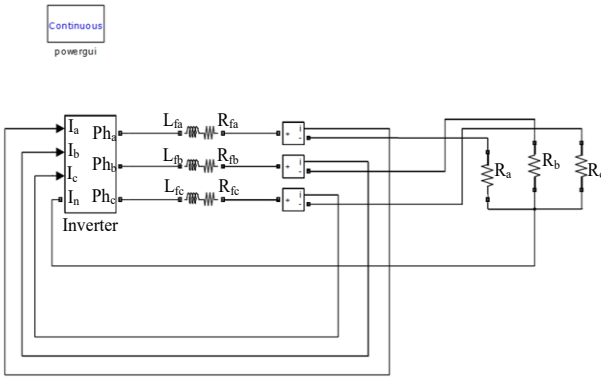

Fig.5 Implemented Matlab/Simulink model of FCS-MPC current control for four-leg VSI.

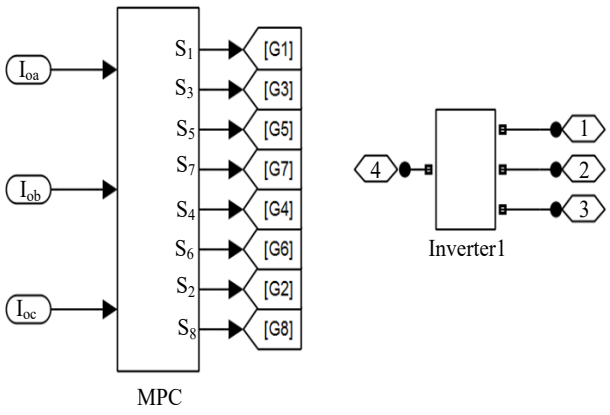

Fig.6 Subsystems contained in inverter subsystem block.

MPC is the second subsystem. The three-phase reference currents generated in this subsystem, with the measured three-phase currents represent the input data, to a Matlab M-file program, which embedded in (mpc1) S-function block. The program executes the FCS-MPC algorithm described earlier, see Fig.4.

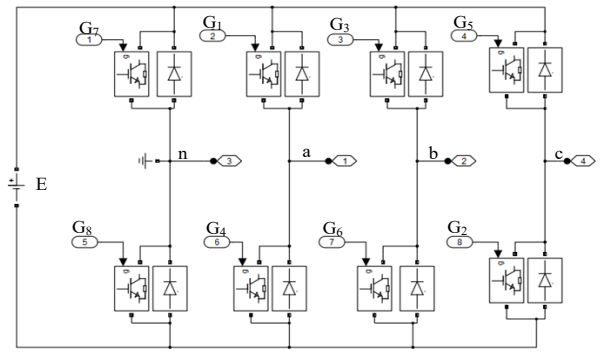

Fig.7 Four-leg inverter subsystem block (Inverter1).

The outputs of the S-function block, provides the switching control signals to the inverter, the inner diagram of this subsystem is shown in Fig.8. These signals represent the switching state that produces an optimal cost function (i.e. minimum error between the predicted and the reference values) at the (k+1) instant.

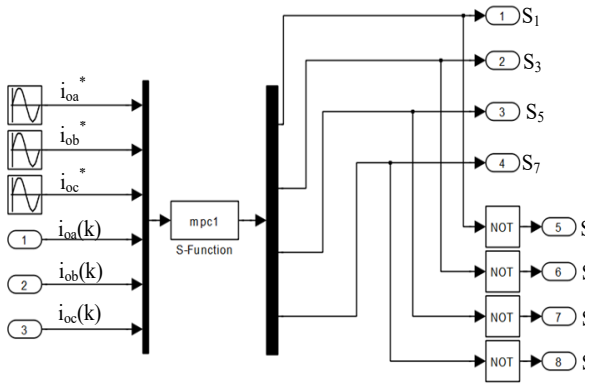

Fig.8 MPC subsystem block.

VI. Simulation Results

Matlab/Simulink program is used to simulate the FCS-MPC current control, based on cost function optimization with current limit constraint for four-leg VSI. The simulation is implemented with balanced and unbalanced loads, steady state and transient conditions, minimum absolute cost function is considered. The three-phase output voltages, load currents, and neutral current In for balanced load, are shown in Figs.9-11. These figures demonstrate the main features of the four-leg inverter and the validity of the proposed algorithm to control this type of inverters.

Figures 12-14 show a comparison between the output load currents and the reference currents. As seen in these figures the predicted output load currents tracks the reference currents precisely, and appear to be almost identical. The inverter output voltages, before the L-R filter stage are shown in Fig.15.

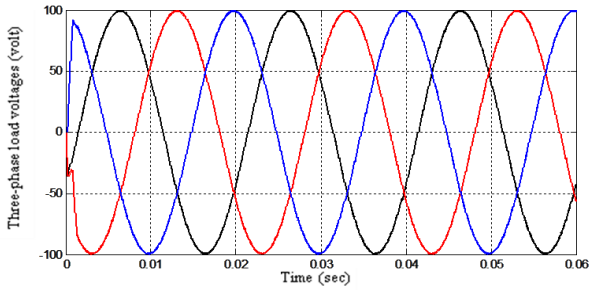

Fig.9 Three-phase output load voltages.

The inverter output voltages vector trajectory, in α, β, and γ coordinates, are shown in Fig.16, this figure shows the outperformance of the proposed algorithm and its similarity to the SVPWM, the voltage vector takes circular shape when the load is balanced.

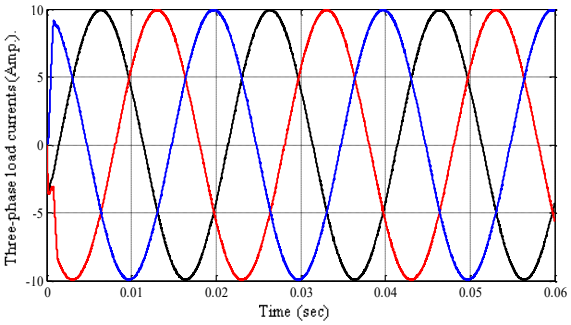

Fig.10 Three-phase output load currents.

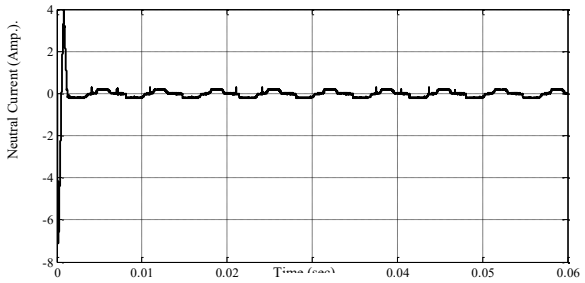

Fig.11 Neutral current In.

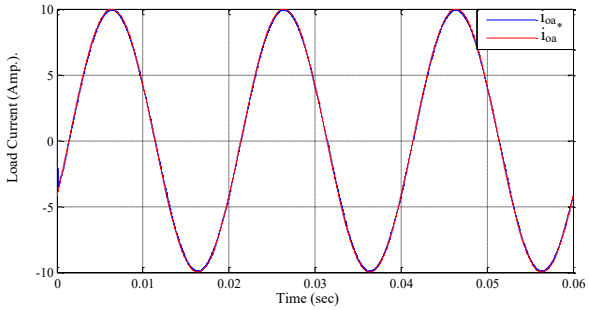

Fig.12 Output load current (in blue) and reference current (in red) for phase a.

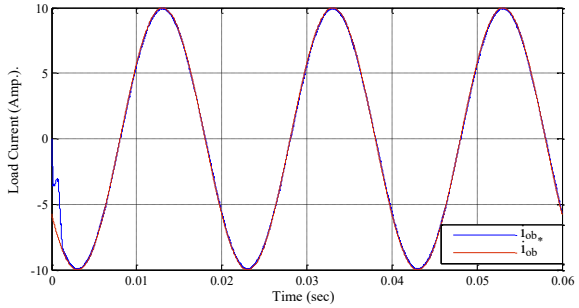

Fig.13 Output load current (in blue) and reference current (in red) for phase b.

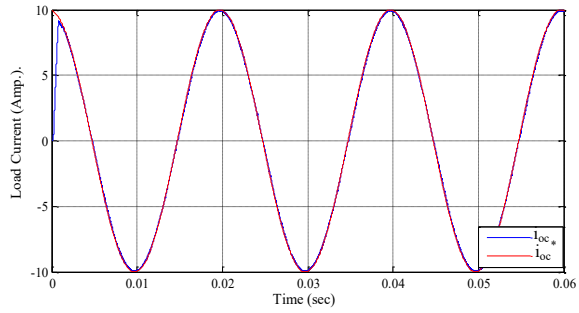

Fig.14 Output load current (in blue) and reference current (in red) for phase c.

As discussed in the previous section, the algorithm selects optimal switching state that produces minimum cost function this is shown in Fig. 17. Figure 18 shows the total harmonic distortion of the inverter output voltage, for SVPWM and FCS-MPC algorithm, with the same load and filter parameters. The simulation result shows clearly the superiority of the proposed FCS-MPC algorithm with less THD by 10%.

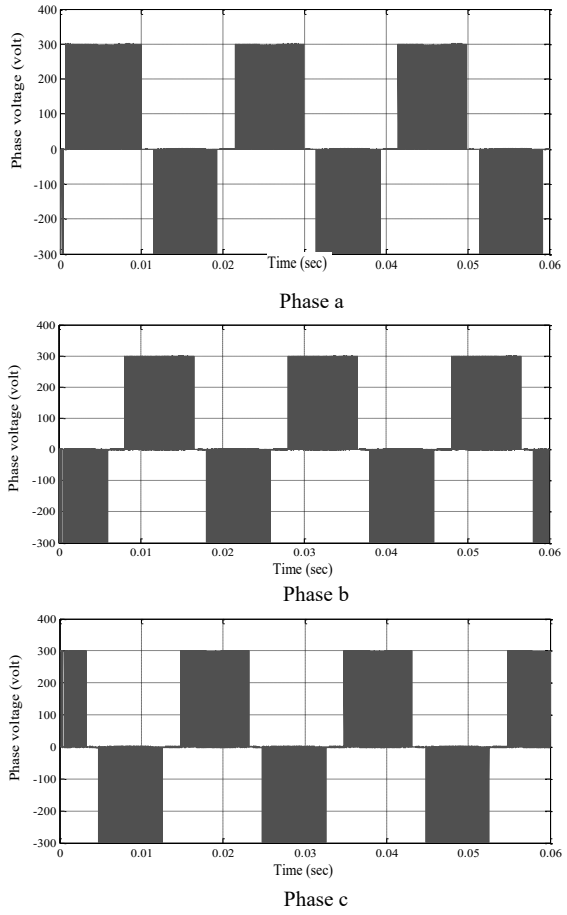

Fig.15 Inverter output voltages before the filter.

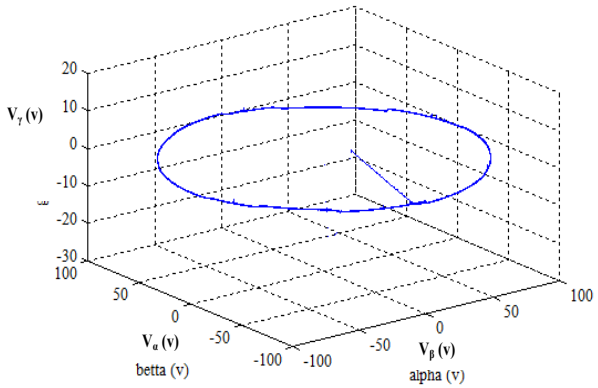

Fig.16 Inverter output voltages vector trajectory in (α, β, and γ coordinates).

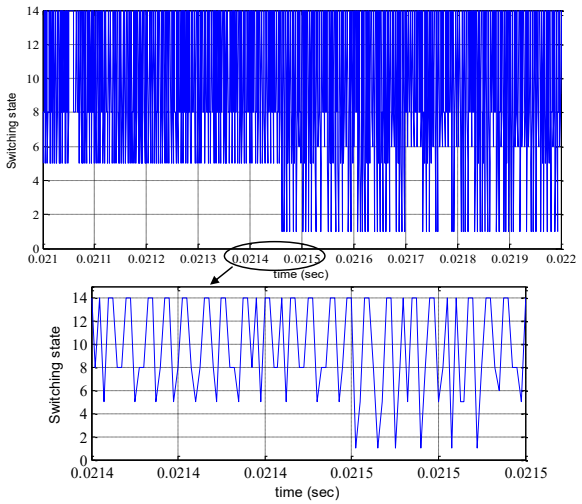

Fig.17 Optimal applied switching states.

To confirm the validity and the robustness of the FCS-MPC current control with current limits constraint two cases are considered, the first is simulation with unbalanced reference currents with balanced loads. The three-phase load currents for this condition are shown in Fig.19. The presented result shows that, although the existences of balanced loads, the three-phase load currents follow the unbalanced reference currents.

Figure 20 show the comparison between the reference currents and the load currents with unbalanced reference currents and balanced load currents condition. The presented results show that load currents match completely with the reference currents. The neutral current is shown in Fig.21, this current acts like the neutral current for unbalanced load.

The second simulation approach is with balanced reference currents and unbalanced loads.

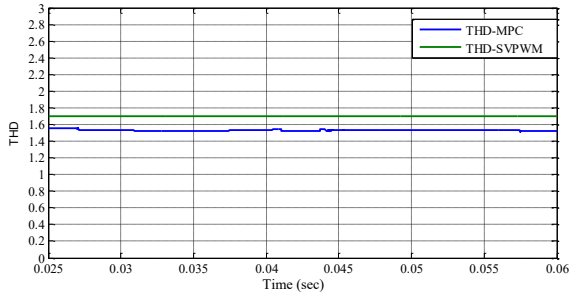

Fig.18 THD for FCS-MPC and SVPWM.

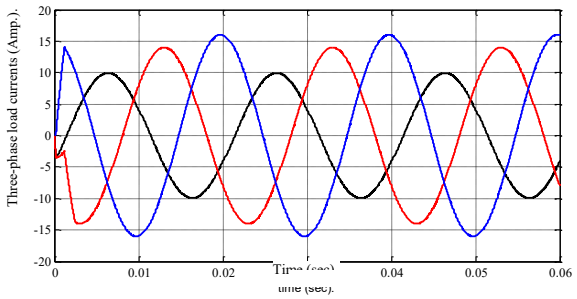

Fig.19 Three-phase output load currents with balanced loads and unbalanced reference currents.

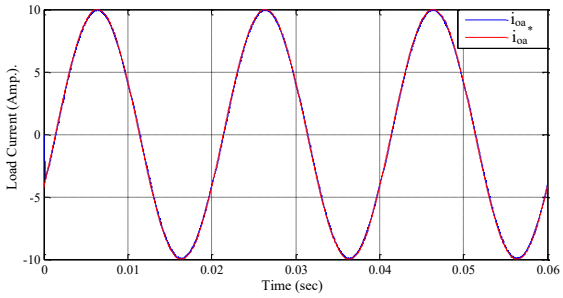

Phase a

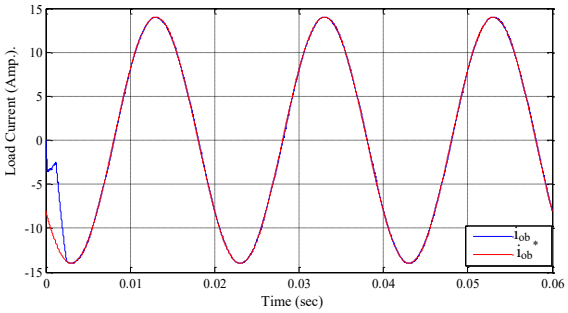

Phase b

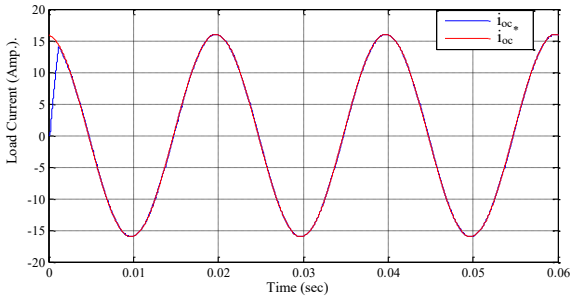

Phase c

Fig.20 Output load current (in blue) and reference current (in red) with balanced load and unbalanced reference currents condition.

In Fig.22, three-phase load currents are shown, although unbalanced load is used in simulation,

balanced three-phase load currents are observed, since the load currents track the balanced reference currents. Figure 23 shows a comparison between the reference currents and the load currents with balanced reference currents and unbalanced load currents condition. The presented results show that load currents match the reference currents in this condition. The neutral current is shown in Fig.24, this current acts like the neutral current for balanced load.

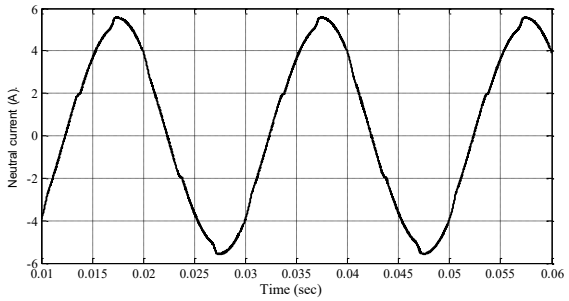

Fig.21 Neutral current with balanced load and unbalanced reference currents.

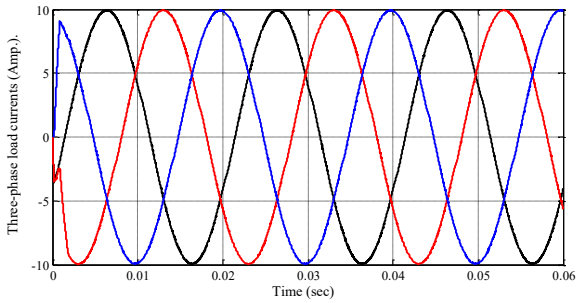

Fig.22 Three-phase output load currents with unbalanced loads and balanced reference currents condition.

The final case study is the step change in reference currents. Figure 25 show the reference current with output load current for the three phases.

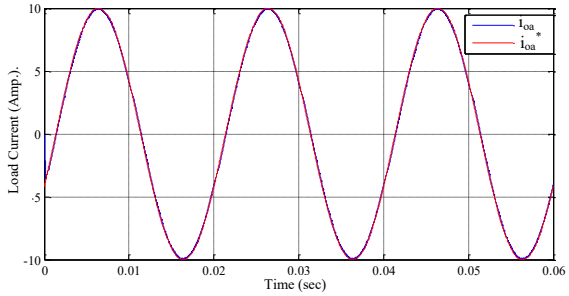

Phase a

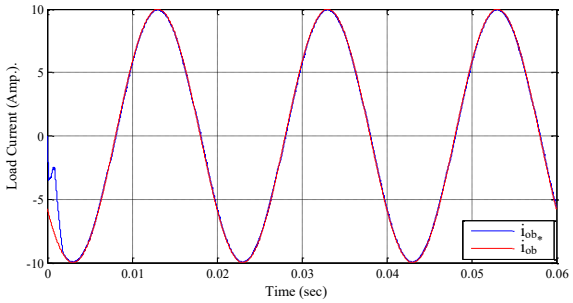

Phase b

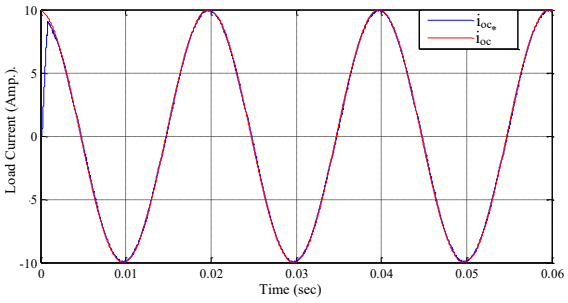

Phase c

Fig.23 Output load current (in blue) and reference current (in red) with unbalanced load and balanced reference currents condition.

The load currents track and match the reference currents immediately without any overshoot. The effectiveness of the algorithm is observed, it is robust against the transient step change of the reference currents. The neutral current for the previous condition is shown in Fig.26, this current acts as that for balanced load, except at the step change instant.

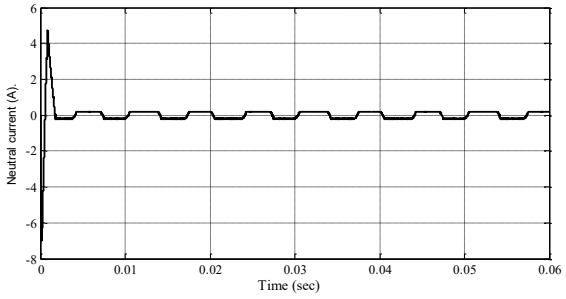

Fig.24 Neutral current with unbalanced load and balanced reference currents.

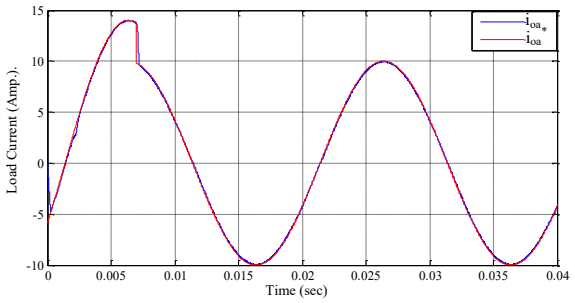

Phase a

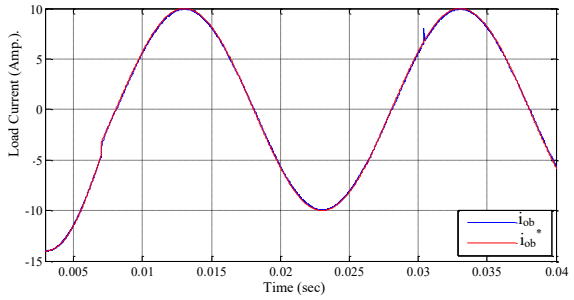

Phase b

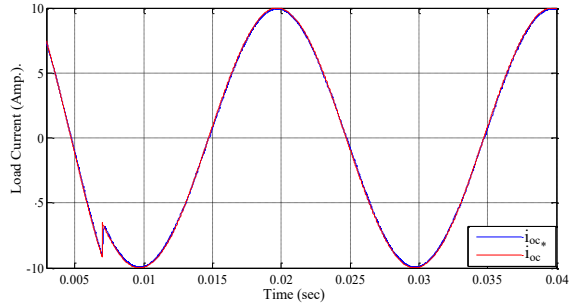

Phase c

Fig.25 Output load current (in blue) and reference current (in red) with step change in reference current.

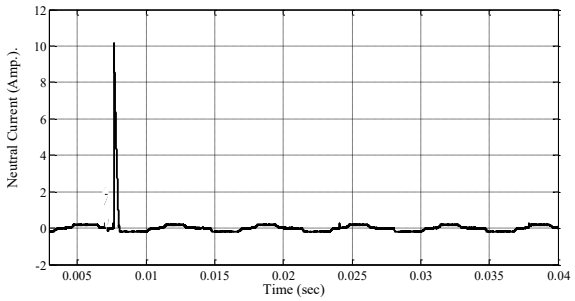

Fig.26 Neutral current with step change in reference currents.

A simple comparison between the results obtained from this new FCS-MPC algorithm and the SVPWM strategy that implemented in the literature[12] can be summarized in Table-2.

Table-2 Comparison between the two performances of FCS-MPC and the SVPWM.

FCS-MPC	SVPWM
1- Simple and easy modeling. 2- The program executing time is fast. 3- Less THD by 10%. 4- Better system response than the SVPWM.	1- Complex and difficult modeling. 2- Long time for executing. 3- Larger THD by 10%.

VII. CONCLUSIONS

In this work a Matlab/Simulink model for the FCS-MPC current control based on cost function optimization, with current limit constraints for four-leg VSI is presented. The algorithm uses the finite possible 16 switching states generated by the four-leg inverter, to predict the load currents at each sampling period. The algorithm compares the predicted currents with predetermined reference currents, and selects the switching state that produces minimum error (minimum cost function). In the next step, the algorithm applies the switching signals that produce optimal switching state, to inverter IGBT switches. The simulation results confirm the validity of that algorithm. Comparison made between the SVPWM and the proposed current predictive algorithm for the same load conditions, the results show the superiority of the new algorithm with observed reduction in inverter output voltage THD.

In addition, a current limit constraint is added to the cost function, which provides better performance to the algorithm, since it eliminates any deviations or overshoots.

Different cases are studied to confirm the robustness and effectiveness of the proposed algorithm, such as balanced loads with unbalanced references, unbalanced loads with balanced references, and transient step change in current references. The simulation results in all the above cases show that the load current track and match its reference without deviations or overshoots.

REFERENCES

[1] J. Rodriguez, and P. Cortes, "Predictive Control of Power Converters And Electrical Drives", a John Wiley & Sons, Ltd. Publication, first edition, 2012, ISBN 978-1-119-96398-1.

[2] A. Almaktoof, A. Raji, and M. Kahn, "Modeling and Simulation of Three-Phase Voltage Source Inverter Using a Model Predictive Current Control", International Journal of Innovation, Management and Technology, vol. 5, no. 1, Feb. 2014.

[3] J. Wang, "Model Predictive Control of Power Electronics Converter", Msc. Thesis, Norwegian University of Science and Technology, pp.1-7, 2012.

[4] T. Geyer, "Low Complexity Model Predictive Control in Power Electronics and Power Systems", PhD. Thesis, Swiss Federal Institute of Technology, 2005.

[5] S. Kouro, P. Cortés, R. Vargas, U. Ammann, and J. Rodríguez, "Model Predictive Control—A Simple and Powerful Method to Control Power Converters", IEEE Trans. on Industrial Electronics, vol. 56, no. 6, Jun. 2009.

[6] J. Rodríguez, J. Pontt, C. Silva, P. Correa, P. Lezana, P. Cortés, and U. Ammann, "Predictive Current Control of a Voltage Source Inverter ", IEEE Trans. on Industrial Electronics, vol. 54, no.1, Feb. 2007.

[7] M. Rivera, V. Yaramasu, J. Rodriguez, and B. Wu, "Model Predictive Current Control of Two-Level Four-Leg Inverters—Part II: Experimental Implementation and Validation", IEEE Trans. on Power Electronics, vol. 28, no. 7, Jul. 2013.

[8] J. Rodriguez, B. Wu, M. Rivera, C. Rojas, V. Yaramasu, and A. Wilson, "Predictive Current Control of Three-Phase Two-Level Four-Leg Inverter", The 14th International Power Electronics and Motion Control Conf. (EPE/PEMC), pp. T3-106 - T3-110, Sept. 2010.

[9] M. Rivera, V. Yaramasu, A. Llor, J. Rodriguez, B.Wu, and M. Fadel, "Digital Predictive Current Control of a Three-Phase Four-Leg Inverter", IEEE Trans. on Industrial Electronics, vol. 60, no. 11, Nov. 2013.

[10] V. Yaramasu, M. Rivera, M. Narimani, B. Wu, and J. Rodriguez, "Model Predictive Approach for a Simple and Effective Load Voltage Control of Four-Leg Inverter with an Output *LC* Filter", IEEE Trans. on Industrial Electronics, vol. 61, no. 10, Oct. 2014.

[11] X. Zhang, T. C. Green, and A. Junyent-Ferr´, "A New Resonant Modular Multilevel Step-Down DC–DC Converter with Inherent-Balancing", IEEE Tans. on Power Electronics, vol. 30, no. 1, Jan. 2015.

[12] Riyadh G. Omar, Rabee' H. Thejel, " Matlab/Simulink Modeling of Four-leg Voltage Source Inverter With Fundamental Inverter output Voltages Vector Observation" Iraqi Journal for Electrical and Electronic Engineering, Vol.11 No.1 , 201 5.